Journal of Materials Science and Engineering A 15 (1-3) (2025) 32-36
doi: 10.17265/2161-6213/2025.1-3.004

# Dynamic Broadband Chiral Response in Mid-infrared via Hybrid Phase-Change Metasurfaces

Yujie Zhang
*Department of Physics, China Jiliang University, Hangzhou 310018, China*

**Abstract:** Chirality is a widespread physical phenomenon in nature, but natural materials often exhibit weak chiroptical responses. Recent advances have used chiral metasurfaces to enhance these responses, with applications in holographic imaging, chiral molecule detection, and circularly polarized lasers. However, most chiral metasurfaces exhibit strong chiroptical responses only at fixed wavelengths, which limits their suitability for wavelength-tunable optical devices. We address this by designing a silicon-GST (silicon-$Ge_2Sb_2Te_5$) hybrid metasurface with asymmetric cross-shaped units that support multi-wavelength resonances, achieving broadband and dynamically tunable CD (circular dichroism). In the amorphous phase, GST enables CD > 0.7 in the range of 2,137 nm to 2,657 nm, with a PER (polarization extinction ratio) up to 38 dB. Upon transition to the crystalline phase, CD enhances with a redshift, and the sign of CD reverses. This enables dynamic wavelength tuning of broadband CD via the phase transition of GST.

**Key words:** Chirality, CD, metasurface, GST.

## 1. Introduction

Chirality refers the geometric property of an object that cannot be aligned with its mirror image via rotation or translation [1]. In optics, chirality is mainly characterized by optical activity and CD (circular dichroism), serving as essential tools for molecular structure research and optical device development [2]. But natural chiral materials have weak chiroptical responses, limiting their practical applications [3]. Metasurfaces, as artificially designed subwavelength structures, can efficiently manipulate electromagnetic wave propagation [4]. By engineering unit cell with chiral features, metasurfaces with chiroptical responses can be created, showing stronger response intensities compared to natural materials [5].

To broaden the application range of chiral metasurfaces, researchers have focused on broadband chiroptical response structures, such as multilayer stacks [6, 7], three-dimensional helical structures [8], and single-layer composite [9, 10]. However, once fabricated, these fixed structures have unchangeable operational wavelength ranges, rendering them unsuitable for multi-wavelength practical scenarios. To address this limitation, tunable chiral metasurfaces, particularly those using phase-change materials like GST ($Ge_2Sb_2Te_5$) with thermally induced non-volatile phase transitions [11, 12], offer a promising solution for reconfigurable chiral optical devices [13, 14].

We propose an asymmetric cross-shaped metasurface based on silicon-GST composite structure, and study the optical properties of this metasurface through numerical simulations. The results show that when GST is in the amorphous state, the structure exhibits significant CD (> 0.7) in the 2,137-2,657 nm wavelength range, with a 520 nm bandwidth. By analyzing the OCD (optical chiral density) distribution, the physical mechanism of broadband chiral resonance is elucidated. Moreover, by modulating the crystalline phase of GST, we have achieved tunable wavelengths and reversible chiral response, while maintaining a 371 nm broadband in the crystalline state. This research offers a viable

**Corresponding author:** Yujie Zhang, M. Eng., research fields: Micro-nano Photonics, Metasurface.

solution to address the functional limitations of conventional chiral metasurfaces and has potential applications in optical communications and sensing.

## 2. Design and Simulation

We presented a composite dielectric metasurface using phase-change material GST, as depicted in Fig. 1a. The metasurface consists of a silica substrate and periodically arranged asymmetric cross-shaped meta-atoms. As illustrated in Fig. 1b, each meta-atom features a GST layer (thickness $H_{GST}$) sandwiched between two symmetric silicon dielectric layers, yielding a total thickness $H$. The detailed geometry of the cross-shaped meta-atom, shown in Fig. 1c, comprises a rectangular bar with length matching the lattice period $P$ and width $L_2$, accompanied by two smaller rectangular blocks of dimensions $W$ and $L_1$ positioned with a center offset of $X$. This intentionally asymmetric layout breaks in-plane mirror symmetry while maintaining $C_2$ rotational symmetry, thereby generating strong chiroptical responses.

The chiroptical properties of the cross-shaped array were analyzed through the commercial software COMSOL Multiphysics. Periodic boundary conditions were applied along the $x$- and $y$-directions, while a perfectly matching layer was implemented in the $z$-direction. Circularly polarized light, generated through orthogonal linear polarization superposition, was normally incident along the $z$-axis. The complex dielectric constants of silicon and silica were adopted from Palik's experimental data [15], with those of amorphous and crystalline GST sourced from Ref [16]. The meta-atom dimensions were specified as: $P$ = 1700 nm, $H$ = 650 nm, $H_{GST}$ = 100 nm, $L_2$ = 250 nm, $W$ = 500 nm, $L_1$ = 400 nm, and $X$ = 150 nm.

Fig. 2a presents the transmission spectra of the cross-shaped metasurface for LCP (left circularly polarized) and RCP (right circularly polarized) light. Across the 2,100-2,650 nm wavelength range, the structure exhibits high transmission for LCP while strongly suppressing RCP transmission, demonstrating remarkable polarization-selective characteristics. Fig. 2b displays the Jones matrix transmission spectra, showing dominant cross-polarized transmission (Trl) under LCP illumination while other components approach 0. The maximum polarization selectivity occurs at 2,223 nm with $T_L$ = 0.98 and $T_R$ = 0.02, yielding remarkable CD and PER (polarization extinction ratio) as defined by:

$$CD = \frac{T_L - T_R}{T_L + T_R}$$

$$PER = 10 \times \log(\frac{T_L}{T_R})$$

where $T_L$ and $T_R$ represent the transmission coefficients for LCP and RCP, respectively. As shown in Figs. 2c and 2d, the metasurface maintains CD > 0.7 over a 520 nm bandwidth, peaking at 0.96, while achieving PER > 17 dB throughout the operational band with a maximum

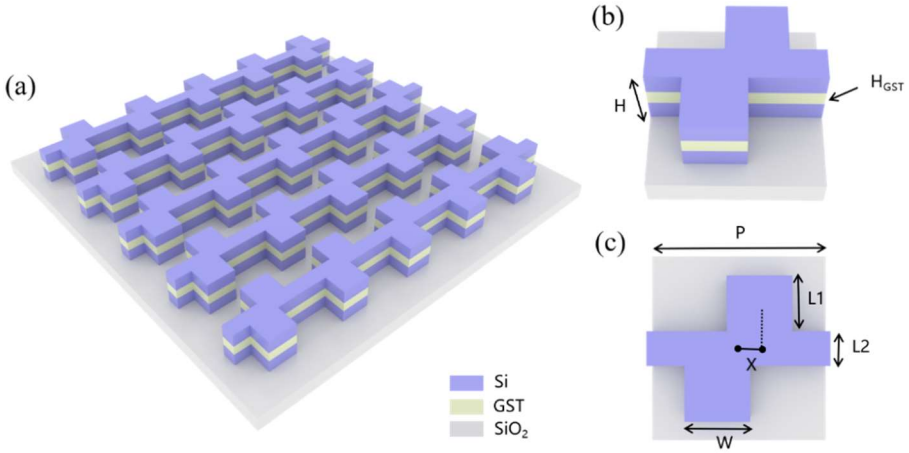


**Fig. 1 Schematic illustration of the cross-shaped chiral metasurface: (a) periodic array configuration, (b) unit cell structure, and (c) top view of the unit cell.**

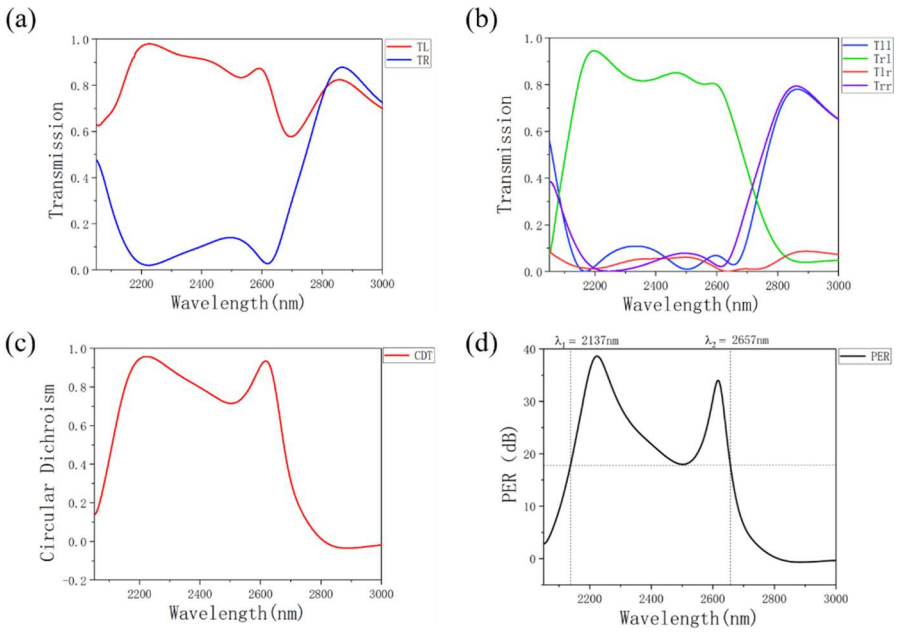


**Fig. 2 The cross-shaped chiral metasurface's: (a) total transmittance, (b) transmittance components, (c) CD, and (d) PER.**

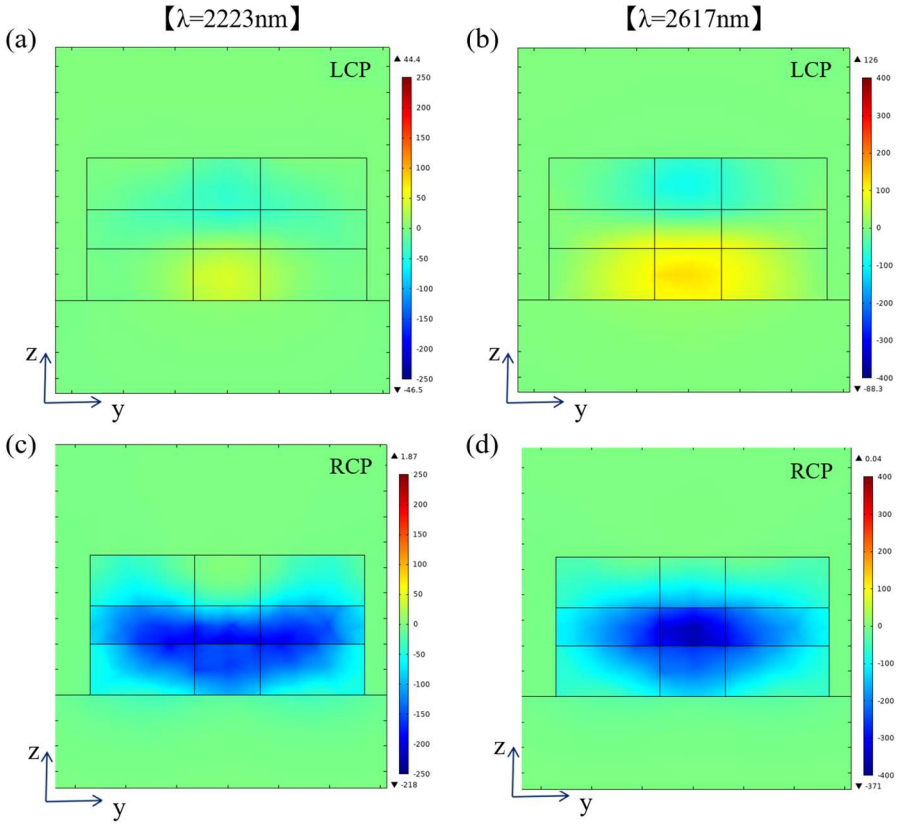


**Fig. 3 Optical chirality density in the cross-shaped chiral metasurface at wavelengths of: (a) (c) 2,223 nm and (b) (d) 2,617 nm.**

of 38 dB at 2,223 nm. These results confirm that the proposed metasurface achieves broadband, highly selective circular polarization control coupled with efficient polarization conversion functionality, providing valuable insights for developing advanced polarization optical devices.

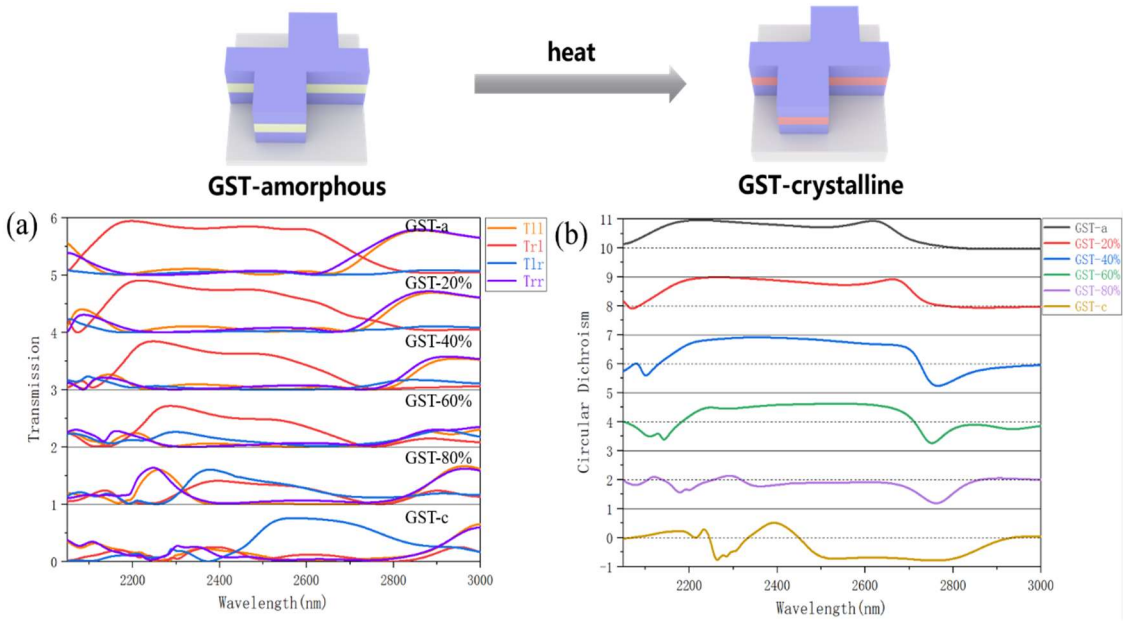


**Fig. 4 (a) transmittance; (b) CD of the cross-shaped chiral metasurface under different GST crystalline phases.**

To elucidate the physical mechanism underlying the chiral response of the metasurface, we calculated the OCD, defined as [17]:

$$OCD = -\frac{\omega}{2} Im(D^* \cdot B)$$

where $\omega$ is the angular frequency, $D^*$ represents the complex conjugate of the electric displacement vector, and $B$ denotes the magnetic flux density. Fig. 3 presents the distribution of OCD at the wavelength of 2,223 nm and 2,617 nm. Analysis of the *y*-*z* sections reveals that the OCD intensity under RCP excitation is significantly higher than that under LCP. This asymmetric distribution directly leads to stronger electromagnetic coupling between RCP and the structure, and formation of a broadband chiroptical response with an average CD > 0.7 across the 2,137-2,657 nm wavelength range. Notably, at 2,223 nm, the spatial coincidence between the localized OCD extremum and the maximum CD value confirms the strong correlation between chiral density distribution and CD.

To investigate the phase-change effect of GST on broadband chiral responses, we analyzed the transmission and CD spectra of the cross-shaped metasurface at various GST crystallization states (amorphous, 20%, 40%, 60%, 80%, crystalline), as shown in Fig. 4. In the amorphous phase, the structure exhibited dominant cross-polarized transmission for LCP light, achieving broadband CD > 0.7 across 2,137-2,657 nm. Phase transition from amorphous to crystalline induced a redshift in chiral resonances due to increasing GST refractive index, expanding the operational bandwidth. Remarkably, crystalline GST generated reversed chirality at 2,572 nm, with RCP cross-transmission (Tlr = 0.75) dominating over LCP (Trl = 0.1), yielding CD = -0.7. As shown in Fig. 4b, the CD > 0.5 over 2,478-2,849 nm with a 371 nm bandwidth, demonstrates switchable chiral responses through GST phase control.

## 3. Conclusions

In this paper, we have demonstrated a phase-change enabled chiral metasurface based on GST-silicon hybrid cross-shaped resonators that achieves switchable broadband chiroptical responses. In the amorphous state, the metasurface exhibits a strong chiral response with CD > 0.7 and PER > 17 dB across 2,137-2,657 nm (520 nm bandwidth), peaking at CD = 0.96 and PER = 38 dB at 2,223 nm. The crystalline

phase induces a red-shifted chiral resonance spanning 2,478-2,849 nm, exhibiting sign-inverted CD with a PER exceeding 10 dB, effectively reversing the optical chirality observed in the amorphous state. This work establishes a viable approach for developing dynamically tunable broadband chiral photonic platforms using phase-change materials.

## References


[1] Khaliq, H. S., Nauman, A., Lee, J. W., and Kim, H. R. 2023. "Recent Progress on Plasmonic and Dielectric Chiral Metasurfaces: Fundamentals, Design Strategies, and Implementation." *Advanced Optical Materials* 11 (16): 2300644.

[2] Hentschel, M., Schäferling, M., Duan, X., Giessen, H., and Liu, N. 2017. "Chiral Plasmonics." *Science Advances* 3 (5): 1602735.

[3] Chen, W., Wang, Z., Gorkunov, M. V., Qin, J. Z., Wang, R. Z., Wang, C. W., Wu, D., Chu, J. R., Kivshar, Y., and Chen, Y. 2024. "Uncovering Maximum Chirality in Resonant Nanostructures." *Nano Letters* 24 (31): 9643-9.

[4] Landy, N. I., Sajuyigbe, S., Mock, J. J., Smith, D. R., and Padilla, W. J. 2008. "Perfect Metamaterial Absorber." *Physical Review Letters* 100 (20): 207402.

[5] Gansel, J. K., Thiel, M., Rill, M. S., Decker, M., Bade, K., and Saile, V. 2009, "Gold Helix Photonic Metamaterial as Broadband Circular Polarizer." *Science* 325 (5947): 1513-5.

[6] Basiri, A., Chen, X., Bai, J., Amrollahi, P., Carpenter, J., Holman, Z., and Yao, Y. 2019. "Nature-Inspired Chiral Metasurfaces for Circular Polarization Detection and Full-Stokes Polarimetric Measurements." *Light: Science & Applications* 8 (1): 78.

[7] Mun, S. E., Hong, J., Yun, J. G., and Lee, B. 2019. "Broadband Circular Polarizer for Randomly Polarized Light in Few-Layer Metasurface." *Scientific Reports* 9 (1): 2543.

[8] Esposito, M., Tasco, V., Todisco, F., Cuscunà, M., Benedetti, A., Sanvitto, D., and Passaseo, A. 2015. "Triple-Helical Nanowires by Tomographic Rotatory Growth for Chiral Photonics." *Nature Communications* 6 (1): 6484.

[9] Wang, R., Wang, C., Sun, T., Hu, X., and Wang, C. 2023. "Simultaneous Broadband and High Circular Dichroism with Two-Dimensional All-Dielectric Chiral Metasurface." *Nanophotonics* 12 (21): 4043-53.

[10] Kang, Q., Xu, G., Zhang, X., Wang, W., Guo, K., and Guo, Z. 2024. "Broadband Mid-Infrared Thermal Emission with Large Degree of Circular Polarization Enabled by Symmetry-Broken Metasurfaces." *Journal of Science: Advanced Materials and Devices* 9 (2): 100724.

[11] Yamada, N. 2012. "Origin, Secret, and Application of the Ideal Phase-Change Material GeSbTe." *Physica Status Solidi (b)* 249 (10): 1837-42.

[12] Du, K. K., Li, Q., and Lyu, Y. B. 2017. "Control over Emissivity of Zero-Static-Power Thermal Emitters Based on Phase-Changing Material GST." *Light: Science & Applications* 6 (1): e16194.

[13] Tang, H., Stan, L., Czaplewski, D. A., Yang, X., and Gao, J. 2023. "Wavelength-Tunable Infrared Chiral Metasurfaces with Phase-Change Materials." *Optics Express* 31 (13): 21118-27.

[14] Cao, T., Wang, R. Z., and Simpson, R. E. 2020. "Photonic Ge-Sb-Te Phase Change Metamaterials and Their Applications." *Progress in Quantum Electronics* 74: 100299.

[15] Palik, E. 1985. *Handbook of Optical Constants of Solids II*, edited by E. D. Palik. New York: Academic Press.

[16] Chew, L. T., Dong, W. L., Lu, L., Zhou, X. L., Behera, J., Liu, H. L., Mao, L. B., Cao, T., Yang, J., and Simpson, R. E. 2017. "Chalcogenide Active Photonics." *Active Photonic Platforms IX. SPIE* 10345: 58-66.

[17] Liang, X., Liang, K., Deng, X., He, C., Zhou, P., Li, J., Qin, J., and Yu, L. 2024. "The Mechanism of Manipulating Chirality and Chiral Sensing Based on Chiral Plexcitons in a Strong-Coupling Regime." *Nanomaterials* 14 (8): 705.